mathematics

MDPI

Article

A Novel Deterministic Probabilistic Forecasting Framework for Gold Price with a New Pandemic Index Based on Quantile Regression Deep Learning and Multi-Objective Optimization

Yan Wang [1] and Tong Lin [2,*]

[1] Haide College, Ocean University of China, Qingdao 266100, China; wangyan2815@stu.ouc.edu.cn
[2] School of Mathematical Sciences, Ocean University of China, Qingdao 266100, China
* Correspondence: lintong@stu.ouc.edu.cn

Abstract: The significance of precise gold price forecasting is accentuated by its financial attributes, mirroring global economic conditions, market uncertainties, and investor risk aversion. However, predicting the gold price is challenging due to its inherent volatility, influenced by multiple factors, such as COVID-19, financial crises, geopolitical issues, and fluctuations in other metals and energy prices. These complexities often lead to non-stationary time series, rendering traditional time series modeling methods inadequate. Our paper presents a multi-objective optimization algorithm that refines the interval prediction framework with quantile regression deep learning in response to this issue. This framework comprehensively responds to gold's financial market dynamics and uncertainties with a screening process of various factors, including pandemic-related indices, geopolitical indices, the US dollar index, and prices of various commodities. The quantile regression deep-learning models optimized by multi-objective optimization algorithms deliver robust, interpretable, and highly accurate predictions for handling non-linear relationships and complex data structures and enhance the overall predictive performance. The results demonstrate that the QRBiLSTM model, optimized using the MOALO algorithm, delivers excellent forecasting performance. The composite indicator AIS reaches −15.6240 and −11.5581 at 90% and 95% confidence levels, respectively. This underscores the model's high forecasting accuracy and its potential to provide valuable insights for assessing future trends in gold prices. The deterministic and probabilistic forecasting framework for gold prices captures the market dynamics with the new pandemic index and comprehensively sets a new benchmark for predictive modeling in volatile market commodities like gold.

Keywords: gold price forecasting; quantile regression; probabilistic prediction models; feature screening; multi-objective optimization algorithms

MSC: 68T07

Citation: Wang, Y.; Lin, T. A Novel Deterministic Probabilistic Forecasting Framework for Gold Price with a New Pandemic Index Based on Quantile Regression Deep Learning and Multi-Objective Optimization. *Mathematics* **2024**, *12*, 29. https://doi.org/10.3390/math12010029

Academic Editor: Ioannis G. Tsoulos

Received: 25 November 2023
Revised: 9 December 2023
Accepted: 18 December 2023
Published: 22 December 2023

1. Introduction

With its multifaceted roles, gold is a pivotal actor in the theatre of the global economy, having intricate interconnections with a spectrum of financial and macroeconomic elements [1,2]. It is a unique asset, with a repository of inherent value beyond its physical commodity aspect, and concurrently orchestrates vital financial and monetary functions within the economic framework [3]. Gold assumes a prominent position in the international reserves across various nations, augmenting its stature and underscoring its universal appeal and strategic significance. Embodied with a triad of characteristics, gold possesses monetary, commodity, and financial properties, outlining its distinctive presence in the economic landscape [4]. During the prevailing dynamism and uncertainties characterizing the global economic milieu, a compelling necessity arises to delve deeply into the strategic implications of gold resources. This involves cultivating a nuanced understanding of the mechanisms that drive the fluctuations in international gold prices, enhancing the precision in forecasting these prices' volatility, and bolstering strategies to safeguard national economic and financial security [5].

The price of gold, which has both commercial and financial attributes [6], is not only influenced by the US dollar exchange rate and the prices of other metals but also by epidemics, geopolitical risks, and other factors [7]. In financial markets, gold has long been regarded as a bastion of safety amidst turbulent times [8]. This phenomenon is particularly evident during crises when gold prices often experience significant fluctuations. For instance, during the Global Financial Crisis of 2008, gold prices saw a notable rise as investors sought refuge from the volatility of traditional stock markets. Similarly, the prolonged duration of the COVID-19 pandemic has saturated the investment and business areas [9–11]. Owing to its substantial effects, governments globally have implemented a variety of urgent actions at the beginning of the COVID-19 outbreak [12]. The emergence of the COVID-19 pandemic at the start of 2020 triggered a sharp rise in gold prices, reflecting the uncertainty and economic instability that characterized the global landscape [13]. These examples underscore the sensitivity of gold prices to crisis events, highlighting its role as a "safe-haven" asset during periods of economic and geopolitical distress. This trend offers a unique insight into investor behavior during crises and underscores the enduring value of gold in a diversified investment portfolio. Since the factors are coupled and interrelated, the price fluctuations of non-ferrous metals are highly irregular and non-linear, which makes accurate and robust price forecasting an arduous job [14].

In recent decades, various techniques have been devised to improve the precision of forecasting gold prices. However, most of these methods concentrate on point predictions. Traditional time series models [15], such as ARIMA, require data stationarity and may struggle with complex trends or seasonal patterns [16]. Machine learning and deep learning [17] have been extensively and successfully applied to the complexity and non-linearity of gold price data. Liu et al. (2017) [18] used the random forest (RF) algorithm to analyze the variables affecting the price of gold and to predict the price of gold. In addition, applying heuristic algorithms to optimize the model parameters is likewise an efficient way to boost the model performance. Weng et al. (2020) [19] proposed a Genetic Algorithm Regularized Online Extreme Learning Machine that can accurately predict the price of gold. Zakaria et al. (2019) [20] proposed the WOA-NN model using the whale optimization algorithm (WOA) [21] as an instructor for learning the multilayer perceptron neural networks, which outperforms the classical NN, particle swarm optimization-neural network [22], genetic algorithm-neural network [23] and ARIMA models.

All the above models' point forecasting performance diminishes under extreme uncertainty conditions [24]. In the face of the complex volatility of the gold price, it should not simply be set to a specific value but to a growth interval that allows more scope for dealing with future uncertainties [25]. In addition, interval forecasting can accurately measure the variability in forecasts due to uncertainty and determine a prediction interval at a certain level of significance that incorporates possible upper and lower bounds on the initial value. This approach provides fuller information and gives more credibility to the predictions [26]. Quantile regression (QR) has been introduced for deterministic and probabilistic range predictions [27]. Unlike ordinary regression, QR is highly sensitive and robust to outliers in the response variable. Also, it exhibits flexibility due to having no strict requirement for normality and homoscedasticity and offers a comprehensive view of the examined relationship with highly interpretable results. Due to its robustness to outliers and the straightforward interpretation of its output parameters through distribution evaluation, QR has become a powerful tool for interval prediction.

QR and interval forecasting are methods with the advantage of parametric interpretability. However, they rely heavily on specific assumptions regarding how the data are generated. Utilizing learning techniques allows for a shift away from these models based heavily on assumptions, moving towards methods more driven by the actual data. These techniques can capture complex non-linear relationships and identify hidden patterns and interactions in data. Models based on neural networks have been utilized to simulate and predict gold prices [28]. Also, Yurtsever et al. (2019) [29] predicted the gold price using LSTM, bi-directional LSTM (BiLSTM) [30], and gated recurrent unit (GRU) [31] methods. These models can capture temporal dependencies in the data, learning patterns over sequences of inputs. However, these intense machine-learning models are frequently regarded as "black boxes", which makes them challenging to interpret and comprehend. Integrating QR and machine-learning methods effectively offers enhanced predictive power, robustness to outliers, the ability to handle complex relationships, and improved interpretability. This fusion provides a comprehensive understanding of data patterns with superior interpretability, leading to more accurate and reliable models. Combination models are proficient at identifying complex patterns within sequential data. However, their predictive performance can be improved further by optimizing the coverage rate and width of the confidence intervals.

Prediction intervals play a crucial role in interval forecasting models, embodying optimal attributes when they satisfy two fundamental conditions. First, they should guarantee a dependable coverage rate for finite samples, and second, they should aspire to minimize the prediction interval width as much as possible [32]. Utilizing multi-objective optimization algorithms to optimize the prediction interval coverage rate and interval width concurrently enhances the precision and reliability of predictions. These algorithms facilitate a balanced trade-off by ensuring that the prediction intervals are neither excessively broad nor overly narrow, allowing for improved accuracy [33]. This approach fosters the development of prediction models that are both reliable and effective, catering optimally to the intrinsic complexities and variances within the data.

This study proposes a novel comprehensive framework designed for forecasting the gold price, emphasizing the pivotal role of gold and its price sensitivity to various determinants such as epidemics, economic flux, and geopolitical uncertainties. The framework combines QR with advanced deep-learning models and further enhances these models using multi-objective optimization algorithms to enhance the prediction's reliability and resolution. Similarly, to other ensemble machine-learning algorithms, this forecasting approach achieves high levels of accuracy and stability but with limited interpretability. To this end, our study incorporates an epidemic index, a geopolitical index, and the US dollar index within the proposed forecasting framework, aiming to significantly enhance its interpretability and practical utility. Though these indices cover significant ground, it is essential to acknowledge that there are numerous other factors influencing gold price volatility that are not currently accounted for in our framework. Looking ahead, our model's feature selection module is designed to be adaptable and universal, enabling the incorporation of additional influential factors in future framework iterations. The forecasting framework demonstrates remarkable resilience and precision, highlighting its capacity to deliver dependable and actionable insights, which are invaluable for investors and policymakers. Also, it effectively captures the dynamic nature of the financial market, making it highly versatile and applicable across a broad spectrum of uses. Key contributions of this research are delineated as follows:

(1) This research presents a robust method for accurate gold price prediction, which is essential due to gold's impact on global commodities and economic indicators like exchange rates. Our approach enhances financial forecasting and serves as an early warning system for potential economic crises. It offers valuable insights for understanding and managing market uncertainties.

(2) Historical crises, with a notable example being the recent pandemic, heavily influence gold prices, highlighting the importance of carefully choosing index variables in predictive model construction for precise forecasts. This study introduces a variable selection method for accurate gold price prediction, accounting for the impact of crises like the recent pandemic. It effectively incorporates both "hard" indicators (metal and energy prices) and "soft" indicators (pandemic and geopolitical indices) using

correlation analysis and economic principles. This approach improves the model's interpretability and relevance in economic contexts.

(3) This approach combines QR and deep-learning models to achieve multivariate probability forecasting. It reaches a balance between interpretability and predictive power. This method enhances the definition of the dependent variable's distribution, significantly improving prediction accuracy.

(4) A novel interval prediction framework proposes the combination of multi-objective optimization with quantile deep learning to forecast gold prices. It optimizes the convergence and width of prediction intervals for enhanced trustworthiness and precision. Experimental results highlight the improved predictive power of the two multi-objective optimization algorithms, leading to more reliable interval predictions.

The subsequent sections of this research are as follows: The probabilistic interval model, evaluation metrics, and MOOA used in this research are presented in Section 2. Two experiments were carried out in this research, and the analysis of the outcomes is given in Section 3. Section 4 outlines the conclusions of this research.

2. Methodology

This research develops a comprehensive forecasting framework for precise gold price predictions by embracing its intrinsic financial characteristics, which have a significant bearing on major commodities and pivotal financial-economic variables like exchange rates. The framework serves as an early warning mechanism for potential economic downturns and a navigator through market uncertainties. Acknowledging the impact of historical crises on gold prices, with a notable example being the recent pandemic, this research framework involves meticulous consideration of various factors and the apt selection of variables. The variable selection methods in this study adeptly select both "hard" indicators, like prices of different metals and energy, and "soft" indicators, such as pandemic and geopolitical indices, enhancing the model's interpretability and relevance in economics. Utilizing probabilistic forecasting algorithms amplifies the accuracy of interval predictions, offering a nuanced understanding of fluctuating contributing factors. The novel framework introduces multi-objective optimization to optimize the convergence and width of prediction intervals, thereby elevating the reliability and precision of interval predictions for gold prices. Through the synergy of these innovative approaches, this work significantly bolsters the accuracy and dependability of forecasting gold prices, contributing substantial insights for navigating economic conditions and market uncertainties.

2.1. Variable Selection

Variable selection is a pivotal phase in model building and is vital for enhancing the model's forecasting accuracy and interpretability. In the realm of gold price forecasting, variable selection has emerged as a cornerstone, instrumental in cultivating models that are both potent and precise. Gold prices are susceptible to many influences, such as the US dollar index, the prices of other metals, the geopolitical index, and the COVID-19 index necessitating a meticulous selection of variables to encapsulate these multifaceted determinants effectively. Employing techniques such as the least absolute shrinkage and selection operator (LASSO) and the Pearson correlation coefficient (PCC) has proven essential. With its prowess in shrinking coefficients and setting them to zero, LASSO facilitates the exclusion of irrelevant variables, mitigating the curse of dimensionality and enhancing model interpretability. This becomes particularly pertinent given the plethora of potential variables that could influence gold prices, ensuring that the model remains robust and less susceptible to overfitting. On the other hand, the Pearson correlation coefficient (PCC) unveils the linear relationships between features. Understanding such linear dependencies is invaluable in the context of gold prices, as it allows for the discernment of variables that significantly sway the prices, ensuring that the model is attuned to the most influential factors.

2.1.1. Least Absolute Shrinkage and Selection Operator (LASSO)

LASSO [34] is a technique for shrinking the dimensionality of data based on absolute coefficients. The essence is to compress the coefficients of the variables by incorporating a penalty term to the traditional objective function so that the aggregate of their absolute magnitudes does not exceed a predefined limit. Also, this method allows for the regression coefficients of specific variables to be set to zero, thus excluding these variables and realizing the effect of dimensionality reduction. The retained variables are considered significant. LASSO regression analysis can effectively decrease the dimensionality of the input variables and solve the multicollinearity problem between variables, thus improving the model's efficacy. The designated equation is presented as follows:

Assuming there are n sets of independent variables with X_i $(i = 1, 2, \cdots, n)$ and dependent variables with Y_i $(i = 1, 2, \cdots, n)$, the equation of LASSO regression is

$$\hat{\beta}_{Lasso} = \underset{\beta}{\operatorname{argmin}} \|Y_i - X_i\beta\|^2 \text{ s.t. } \sum_{i=1}^{n} |\beta_i| \leq q,\ q \geq 0 \tag{1}$$

equivalent to

$$\hat{\beta}_{Lasso} = \underset{\beta}{\operatorname{argmin}} \left(\|Y_i - X_i\beta\|^2 + \lambda \sum_{i=1}^{n} |\beta_i| \right) \tag{2}$$

In Equation (2), $q \geq 0$ is the adjustment parameter, which affects the accuracy of the parameter estimates; β_i is the regression coefficient; λ is the non-negative regularization coefficient; and $\lambda \sum_{i=1}^{n} |\beta_i|$ is called the penalty term.

2.1.2. Pearson Correlation Coefficient (PCC)

The PCC [35] is a linear correlation coefficient mainly applied to define the extent of linear correlation between different features. Overall, the following formula allows for the computation of the correlation coefficient:

$$\rho_{X,Y} = \frac{E((X - EX)(Y - EY))}{\sqrt{Var(X)}\sqrt{Var(Y)}} \tag{3}$$

where E represents the mathematical expectation of the variable, i.e., the mean; Var means the variance of the variable, and $\sqrt{D}$ means the standard deviation of the variable; $E((X - EX)(Y - EY))$ represents the covariance between the random variables X and Y; and $\rho_{X,Y}$ represents the ratio of the covariance and standard deviation between random variables X and Y.

Estimating the correlation coefficient r amidst X and Y can be obtained by calculating their covariance and standard deviation as follows:

$$r = \frac{\sum_{i=1}^{n} \left(X_i - \overline{X}\right)\left(Y_i - \overline{Y}\right)}{\sqrt{\sum_{i=1}^{n} \left(X_i - \overline{X}\right)^2} \sqrt{\sum_{i=1}^{n} \left(Y_i - \overline{Y}\right)^2}} \tag{4}$$

The value of r ranges from $[-1, 1]$. The nearer its absolute magnitude is to 1, the more potent the correlation between the variables, and the closer it is to 0, the weaker the relationship between the variables.

In conclusion, variable screening using LASSO and the PCC is an effective strategy in gold price forecasting. LASSO's dimensionality reduction capability ensures model refinement to focus on the most influential variables, promoting a nuanced understanding of gold price influences. Simultaneously, the PCC elucidates the linear interdependencies among variables, enabling the model to be finely tuned to the intricacies of market dynamics. The synergistic integration of these variable-screening methods prepares the forecasting model, ensuring it can adeptly navigate the complexity and uncertainty of the gold market, ultimately producing accurate and reliable forecasts.

2.2. Probabilistic Prediction Models

Quantile regression models accurately capture intricate gold price movements and information sensitive to the various factors affecting the gold price. Deep learning has increased across diverse sectors, establishing itself as a leading approach for forecasting the financial market [36]. Our framework merges quantile regression with deep learning to improve interval forecasting, ensuring precise prediction of interval endpoints. This synergy, first discussed in seminal works [37], leverages neural networks to sidestep rigid data distribution assumptions, crucial for tail distribution estimation. This fusion captures intricate non-linear patterns, enhancing model flexibility and structural determination. Its significant impact on risk management and financial forecasting is underscored by compelling numerical results. This section will emphasize the quantile regression long short-term memory model (QRLSTM) and the quantile regression bidirectional long short-term memory model (QRBiLSTM), highlighting the integration of QR with various machine-learning algorithms.

2.2.1. Quantile Regression (QR)

The principle of QR [38] is to split the data into several quantile points based on the magnitude of the reliant variable and then to study the regression effect on these quantile points separately. The QR method not only analyzes the conditional expectations of the explanatory variable but also the correlation between the analytical variable and the median and quantile of the distribution of the descriptive variable. Median regression is a specific instance of QR where the minimization of residuals is achieved using symmetric weights. At the same time, the other conditional QR requires asymmetric weights to solve the residual minimization. The linear quantile regression model is calculated as follows:

$$Q_{Z_t}(\tau|\Lambda_t) \triangleq F\left(\Lambda_t, \overset{=}{\zeta}(q)\right) = \Lambda_t \overset{=}{\zeta}(q) \tag{5}$$

where $\overset{=}{\zeta}(q) = (\zeta_0(q), \zeta_1(q), \cdots, \zeta_m(q))$ is the regression coefficient matrix, when $\tau = q$, i.e., $Q_{Z_t}(q|\Lambda_t)$ represents the conditional quantile of level q. The predicted value $\hat{\overset{=}{\zeta}}(q)$ of $\overset{=}{\zeta}(q)$ is determined as follows:

$$\hat{\overset{=}{\zeta}}(q) = \operatorname{argmin}\left(\sum_{t=1}^{n} \Psi_q\left(Y_t - \Lambda_t \overset{=}{\zeta}(q)\right)\right) \tag{6}$$

$$\Psi_q\left(Y_t - \Lambda_t \overset{=}{\zeta}(q)\right) = \begin{cases} (1-q)\left(Z_t - \Lambda_t \overset{=}{\zeta}(q)\right), & Z_t - \Lambda_t \overset{=}{\zeta}(q) < 0 \\ q\left(Z_t - \Lambda_t \overset{=}{\zeta}(q)\right), & Z_t - \Lambda_t \overset{=}{\zeta}(q) > 0 \end{cases} \tag{7}$$

The following expression estimates the q-th conditional quartile of the dependent variable:

$$Q_{Z_t}(q|\Lambda_t) \sim \Lambda_t \hat{\overset{=}{\zeta}}(q) \tag{8}$$

2.2.2. Quantile Regression Long Short-Term Memory (QRLSTM)

LSTM is based on recurrent neural networks (RNNs) and has memorability and parameter sharing features [39]. LSTM neural networks can productively learn long-term dependencies between different data sequences and better handle the gradient problem that may exist when training neural networks. Over the years, scholars have made various improvements to LSTM to provide more scientific analysis results for data exhibiting short- or long-term dependencies. QRLSTM is a fusion of QR and LSTM that solves the problem of non-linearity involving temporal information and quantifies the ambiguity of prediction. For quantile q, the QRLSTM is calculated as follows:

$$\begin{cases} M_{t,q}^{L} = \vartheta\left(V_{M_{t,\,q}^{L}} \cdot \left[X_{n,t}, I_{t-1,q}^{L}\right]\right) \\ F_{t,q}^{L} = \vartheta\left(V_{F_{t,\,q}^{L}} \cdot \left[X_{n,t}, I_{t-1,q}^{L}\right]\right) \\ A_{t,q}^{L} = F_{t,q}^{L} \times A_{t-1,q}^{L} + M_{t,q}^{L} \times \tanh\left(V_{U^{L},q} \cdot \left[X_{n,t}, I_{t-1,q}^{L}\right]\right) \\ \Phi_{t,q} = \vartheta\left(V_{\Phi,q} \cdot \left[X_{n,t}, I_{t-1,q}^{L}\right]\right) \\ I_{t,q}^{L} = \Phi_{t,q} \times \tanh\left(A_{t,q}^{L}\right) \\ y_{n,t,q}^{L} = \vartheta\left(V_{L,q} \cdot I_{t,q}^{L}\right) \end{cases} \tag{9}$$

In Equation (9), [ ] denotes two vectors joined together, the symbol $\times$ denotes matrix multiplication, and $\cdot$ means the product of matrix elements. $W_{\cdot\,,\,q}$ denotes a vector of parameters for a particular cell. $M_{t,q}^{L}$ and $F_{t,q}^{L}$ represent the forgetting gate and the input gate, respectively. $\vartheta(\cdot)$ is the sigmoid activation function, and $\tanh(\cdot)$ is the tanh activation function, respectively. $\Phi_{t,q}$ is the output gate multiplied, and $A_{t,q}^{L}$ is the storage. $I_{t,q}^{L}$ is the final update information obtained using the activation function $\tanh(\cdot)$. The last dense layer absorbs $I_{t,q}^{L}$ and correlates it with the parameter $V_{L,q}$, resulting in a quantified prediction $y_{n,t,q}^{L}$.

The integration of QR and LSTM networks enhances the forecasting capabilities; QR is robust to outliers and captures the central tendency of the predicted distribution, and LSTM excels in handling continuous data and effectively captures the temporal dynamics. In particular, QRLSTM utilizes the advantages of LSTM in handling time series data compared to QR and QRNN and is more suitable for predicting the nuances and uncertainties in the series.

2.2.3. Quantile Regression Bi-Directional Long Short-Term Memory (QRBiLSTM)

Bi-directional LSTM (BiLSTM) [40] is an enhanced iteration of LSTM that employs two independent hidden layers, forward and reverse, to process time series data. In this way, BiLSTM can maximize the use of past and future information for data processing, thus effectively solving the limitation that LSTM can only process data in one direction. The calculation steps are as follows:

$$\begin{cases} f_t = \sigma\left(w_{fxt} + w_{fht-1} + b_f\right) \\ z_t = \sigma(w_{zxt} + w_{zht-1} + b_z) \\ l_t = \sigma(w_{lxt} + w_{lht-1} + b_l) \\ h_t = l_t \cdot \tanh(c_t) \\ \hat{y}_t = f\left(w_{yx} \cdot h_t + b_y\right) \end{cases} \tag{10}$$

In Equation (10), f_t determines which part of the history information is eliminated, producing values in the range 0 to 1. z_t determines which data should be fed into the network, making output values in the range of 0 to 1. l_t determines which network outputs are utilized as the final output and which contents of the current cell should be transmitted to the hidden layer h_t, with output values from 0 to 1. $\hat{y}_t$ is an expression for the predicted output.

The output of the BiLSTM model is assumed to be

$$Q_{Y_k}(X_k) = f(X_k, \Psi) \tag{11}$$

where Ψ is the parameters of the BiLSTM model. The QRBiLSTM model can be expressed as follows:

$$Q_{Y_k}(\tau|X_k) = f(X_k, \Psi(\tau)) \tag{12}$$

Combining QR with BiLSTM networks creates a powerful forecasting model adept at capturing past and future data dependencies. This union enhances the model's ability to understand and leverage temporal sequences in the data. Compared to QRLSTM, QRBiLSTM utilizes information from both directions in time, improving predictive accuracy.

2.3. Evaluation Metrics

In this study, the prediction interval coverage probability (PICP) is used as a measure of reliability, the prediction interval normalized average width (PINAW) is used as a measure of resolution, and the average interval score (AIS) is used as a composite metric to evaluate the precision of interval prediction comprehensively [41]. Further, this study also used semi-interval metric (SIM) and quantile loss (QL) to assess the model.

(1) Prediction Interval Coverage Probability (PICP)

PICP refers to the likelihood that the prediction interval contains actual data and is used to characterize the reliability of the interval prediction result. The equation is computed in the following manner:

$$PICP^{(\alpha)} = \frac{1}{n}\sum_{i=1}^{n} \xi_i^{(\alpha)},\ \xi_i^{(\alpha)} = \begin{cases} 1,\ y_i \in \left[L_i^{(\alpha)}, U_i^{(\alpha)}\right] \\ 0,\ y_i \notin \left[L_i^{(\alpha)}, U_i^{(\alpha)}\right] \end{cases} \tag{13}$$

In Equation (13), $L_i^{(\alpha)}$ and $U_i^{(\alpha)}$ represent the highest and lowest limits of the prediction interval, respectively. y_i is the observed value. Interval forecasting confidence levels are taken as $\alpha = 0.05$ and $\alpha = 0.1$. Therefore, the PINC is expressed as $PINC^{(\alpha)} = (1-\alpha) \times 100\%$. If *PICP* > *PINC*, the interval prediction is considered reliable.

(2) Prediction Interval Normalized Average Width

Prediction interval normalized average width refers to the average distance within the range of the lowest and highest value of the forecast interval and is used to measure how much uncertainty is included in the forecast outcome. Also, PICP and PINAW can be considered in combination to prevent the problem of overly conservative interval widths at high interval coverage. The calculation formula is as follows:

$$PINAW^{(\alpha)} = \frac{1}{(y_{t,\max} - y_{t,\min})n}\sum_{i=1}^{n}\left(U_i^{(\alpha)} - L_i^{(\alpha)}\right) \tag{14}$$

(3) Average Interval Score

The AIS is a composite indicator for assessing interval forecasting. The indicator takes into account both PICP and PINAW. The larger the indicator, the better the quality of the forecast interval. Interval scores for the *i*-th interval are

$$S_i^{(\alpha)} = \begin{cases} -2\alpha\left(U_i^{(\alpha)} - L_i^{(\alpha)}\right) - 4\left(L_i^{(\alpha)} - y_i\right) & if\ \ y_i < L_i^{(\alpha)} \\ -2\alpha\left(U_i^{(\alpha)} - L_i^{(\alpha)}\right) & if\ \ y_i \in \left[L_i^{(\alpha)}, U_i^{(\alpha)}\right] \\ -2\alpha\left(U_i^{(\alpha)} - L_i^{(\alpha)}\right) - 4\left(y_i - U_i^{(\alpha)}\right) & if\ \ y_i > U_i^{(\alpha)} \end{cases} \tag{15}$$

Then, the formula for AIS is

$$AIS^{(\alpha)} = \frac{1}{n}\sum_{i=1}^{n} S_i^{(\alpha)} \tag{16}$$

(4) Semi-interval metric

The equations used to assess the PICP for the upper half of the interval, as well as the PINAW, are shown below:

$$PICP_{upper}^{semi}(q) = \frac{1}{N}\sum_{i=1}^{N} \xi_i^{upper},\ \xi_i^{lower} = \begin{cases} 0 & upperquantile_i(q) < y_i \\ 1 & upperquantile_i(q) \geq y_i \end{cases} \tag{17}$$

$$PINAW_{upper}^{semi} = \frac{1}{NR}\sum_{i=1}^{N}(upperquantile_i(q) - y_i) \tag{18}$$

where N is the extent of the test value, R is the span of test values, and $upperquanltile_i(q)$ is the upper bound at the desired level q;

Similarly, the evaluation indicator equation for the lower bound is

$$PICP_{lower}^{semi}(q) = \frac{1}{N}\sum_{i=1}^{n} \xi_i^{lower},\ \xi_i^{upper} = \begin{cases} 0 & lowerquantile_i(q) < y_i \\ 1 & lowerquantile_i(q) \geq y_i \end{cases} \tag{19}$$

$$PINAW_{lower}^{semi} = \frac{1}{NR}\sum_{i=1}^{N}(lowerquantile_i(q) - y_i) \tag{20}$$

(5) Quantile loss (QL)

Quantile loss can be calculated using the following formula:

$$L_t^P(y_t, \hat{y}_{t,q}, q) = \begin{cases} (\hat{y}_{t,q} - y_t) \times (1-q) & y_t < \hat{y}_{t,q} \\ (y_t - \hat{y}_{t,q}) \times q & y_t \geq \hat{y}_{t,q} \end{cases} \tag{21}$$

where $\hat{y}_{t,q}$ is the conditional quantile of the observed value y_t at q quantile, and q is the desired level.

2.4. Multi-Objective Optimization Algorithm

This study employs multi-objective optimization algorithms to enhance its accuracy. Regarding probabilistic forecasting, two crucial assessments are important: reliability and resolution of the prediction intervals. Reliability refers to the consistency and credibility of the model's predictions, ensuring that the prediction intervals accurately reflect the actual uncertainty. Resolution, on the other hand, focuses on the granularity and specificity of the prediction intervals. Using optimization algorithms, the model gains enhanced capabilities to handle the complexity and uncertainty in prediction tasks. These algorithms empower the model to refine its predictions, leading to producing more reliable, accurate, and detailed results. Therefore, with a known quantile, by optimizing reliability and resolution simultaneously through multi-objective optimization algorithms, the aim of the study was to create a more robust and precise probabilistic forecasting model. These algorithms allow the trade-offs between reliability and resolution to be addressed. This approach is vital because enhancing one aspect without considering the other could lead to a model that either overestimates its certainty (high reliability but low resolution) or provides overly cautious and non-specific predictions (high resolution but low reliability). The objective function is as follows:

$$\min\begin{cases} ZDT^{interval} = (1-q) - PICP^{semi}(q) \\ ZDT^{interval} = PINAW^{semi} \cdot \left[1 + e^{(-\delta\cdot(PICP^{semi}(q)-1+q))}\right] \end{cases} \tag{22}$$

where δ is the penalty factor, usually taking a value of 0.05, and the value of the quantile is one of our constraints.

Two multi-objective optimization algorithms, MOALO and MOMVO, were used in this study. To enhance the interval prediction results of the QR deep-learning model for gold price forecasting, the gold price data were split into training, testing, and validation sets at first. Then, the QR deep-learning model was trained using the training dataset. It then made interval predictions on the validation for two sets of quantiles (0.05 and 0.95; 0.025 and 0.975), creating lower and upper bounds of the prediction interval. MOALO and MOMVO algorithms were then employed to optimize the interval predictions from the QR deep-learning model. The aim was to iteratively search for the optimal "interval modification factors" constrained in 0–2 that minimize the objective function, which involves addressing the trade-offs between reliability and resolution. Once the multi-objective optimization algorithms find the optimal solution, the interval modification factors are multiplied on the original QR deep-learning interval predictions. This process adjusts the prediction intervals on the validation set, resulting in optimized intervals that better meet the desired criteria. After that, the final optimized intervals are generated by applying the interval modification factor to the prediction interval on the test dataset.

$$\begin{gathered} Minimize : ZDT^{\text{int}erval} \\ subject\ to : q \in \{0.05, 0.95, 0.025, 0.975\} \\ 0 \leq f \leq 2 \end{gathered} \tag{23}$$

Let q be the quantile used for interval forecasting and f be the interval modification factor produced by the optimization algorithms.

In essence, the multi-objective optimization algorithm refines the initial prediction intervals from the QR deep-learning model by iteratively searching for and applying the best interval modification factors. This results in more accurate and reliable interval predictions for gold prices. The detailed mathematical principles of multi-objective optimization algorithms are demonstrated in the following section.

2.4.1. Multi-Objective Ant Lion Optimizer (MOALO)

Antlion optimization (ALO) [42] is an optimization algorithm inspired by the interaction between ants' hunting behavior and their preferred prey. ALO approximates the global optimal solution as an optimization issue by generating a random set of solutions stepwise. The best solution to a given optimization issue is continuously varying the relationship between ant and colony clusters.

To solve the optimization problem, the ALO algorithm simulates the ants' random walking, becoming trapped in an anthill, building an anthill, sliding towards an anthill beam, capturing prey and reconstructing the anthill, and sliding towards the beam. The anthill and elitism aspects were reconstructed. The mathematical model is shown below.

Assume that the initial wandering position of the ants is as follows:

$$A(k) = [0, cumsum(2g(k_1) - 1), cumsum(2g(k_2) - 1), \cdots, cumsum(2g(k_n) - 1)] \tag{24}$$

$$g(s) = \begin{cases} 1 & if\ \ \rho > 0.5 \\ 0 & if\ \ \rho \leq 0.5 \end{cases} \tag{25}$$

where *cumsum* denotes accumulation; g is a random function; n denotes the highest number of iterations, adjusted to 500 in this study, and population size is also set to 500; s denotes the iteration step size; and ρ is a random number within the span of [0, 1].

Random wandering is normalized to prevent the search space from being exceeded using the following equation:

$$A_i^k = \frac{\left(A_i^k - c_i\right) \times \left(b_i^k - a_i^k\right)}{(d_i - c_i)} + a_i^k \tag{26}$$

where a_i^k and b_i^k denote the smallest and largest values for the random variation in the i-th variable during the k-th iteration. c_i and d_i represent the minimum and maximum limits of the i-th variable during the k-th iteration, respectively.

For changing the random walking behavior around the colony to avoid ants falling into the trap of the colony pit, the equation is expressed below:

$$a_i^k = Antlion_j^k + a^k \tag{27}$$

$$b_i^k = Antlion_j^k + b^k \tag{28}$$

where a^k and b^k are the smallest and largest values of all variables during the k-th iteration, respectively.

For the ants moving into the colony, according to the following formula, the boundary of the random walking will be gradually reduced:

$$a^k = \frac{a^k}{\lambda}, \; b^k = \frac{b^k}{\lambda} \tag{29}$$

where λ is a ratio.

Then, the ants are captured, and the pit is reconstructed, calculated as follows:

$$Antlion_j^k = Ant_i^k \quad if \;\; f\left(Ant_i^k\right) < f\left(Antlion_j^k\right) \tag{30}$$

where Ant_i^k signifies the location of the i-th ant during the k-th iteration.

The elite operator, affecting all ants, is the last operator in ALO and stores the most suitable ants formed during optimization. This means that the selected ant colony (chosen by roulette) and the elite ant colony will attract random walking. Consider the following equations for both:

$$Ant_i^k = \frac{R_W^k + R_E^k}{2} \tag{31}$$

where R_W^k and R_E^k refer to the random fluctuations surrounding the ant that has been chosen through the roulette method and the random fluctuations around the elite, respectively.

To implement the multi-objective problem [43], Equation (30) in the ALO algorithm is modified as follows:

$$Antlion_j^k = Ant_i^k \quad if \;\; f\left(Ant_i^k\right) \prec f\left(Antlion_j^k\right) \tag{32}$$

Another modification is the choice of random ants and elites in Equation (31). We use roulette and Equation (32) to select non-dominated solutions from the archives.

2.4.2. Multi-Objective Multiverse Optimization Algorithm (MOMVO)

According to Mirjalili et al., the multiverse optimizer [44] is a metaheuristic algorithm rooted in the multiverse theory of quantum mechanics. The MVO focuses on three crucial concepts in the multiverse: black holes, white holes, and wormholes. Typically, population-based metaheuristic algorithms comprise two primary stages: exploration and exploitation. In the MVO, the black hole white hole model is used to explore space, and a wormhole is helpful in exploring space.

In the algorithm, the diverse population of the multiverse is composed as follows:

$$U = \begin{bmatrix} y_1^1 & y_1^2 & \cdots & y_1^d \\ y_2^1 & y_2^2 & \cdots & y_2^d \\ \vdots & \vdots & \vdots & \vdots \\ y_n^1 & y_n^2 & \cdots & y_n^d \end{bmatrix} \tag{33}$$

where d is the number of dimensions, fixed as 1, and n is the universe population.

Initially, the universe population was set to 100 in this study and underwent standardization as part of pre-processing. Then, the pre-processed multiverse population was chosen based on random selection probabilities through a method akin to Russian roulette, yielding the subsequent outcomes:

$$y_i^j = \begin{cases} y_k^j & \delta_1 < NI(U_i) \\ y_i^j & \delta_1 \geq NI(U_i) \end{cases} \tag{34}$$

In Equation (34), y_i^j is the j-th star in the i-th universe, $NI(U_i)$ is the normalized universe expansion rate for the i-th universe, δ_1 is a random number that falls within the span of [0, 1], and y_k^j represents the value of the j-th star in the k-th universe, which is calculated using the roulette algorithm.

The MVO determines which universe has a white hole using a roulette algorithm. The Russian roulette algorithm operates based on the normalized expansion rate of each universe. In this algorithm, a universe with a lower expansion rate is assigned a higher probability of its stars being transported to other universes via tunnels formed by black and white holes. When δ_1 is less than the normalized universe expansion rate $NI(U_i)$ for the i-th universe, space-time travel occurs between the i-th universe and the k-th universe, and the star y_i^j at position j in the i-th universe is replaced by the star y_k^j selected by the roulette algorithm.

To ensure that each universe experiences local variations, a high probability of providing higher expansion rates using the wormholes, in which the tunneling of wormholes is established, was created between the best universes in the universe. This mechanism is expressed as

$$y_i^j = \begin{cases} \begin{cases} Y_j + TDR \times \left(\left(ub_j - lb_j \right) \times \delta_4 + lb_j \right) & \delta_3 < 0.5 \\ Y_j - TDR \times \left(\left(ub_j - lb_j \right) \times \delta_4 + lb_j \right) & \delta_3 < 0.5 \end{cases} & \delta_2 < WEP \\ \qquad y_i^j & \delta_2 \geq WEP \end{cases} \tag{35}$$

In Equation (35), WEP refers to the likelihood of the wormhole's presence and is a dynamic parameter; TDR represents the travel distance rate and is also a dynamic parameter; y_i^j is the j-th star in the i-th universe; Y_j is the j-th star in the optimal universe at present; ub_j is the higher limit of all stars in the i-th universe; lb_j is the lower limit of all stars in the i-th universe; and δ_2, δ_3, and δ_4 are random values from 0 to 1.

Equation (35) highlights that WEP and TDR are the two most significant factors establishing the maximum and minimum bounds of individual stars within the universe. However, whereas WEP remains constant, TDR is refined throughout the iterative process to facilitate an accurate exploitation of the optimal universe. The adjustable equations for WEP and TDR are presented below:

$$WEP = WEP_{\min} + t \times \left(\frac{WEP_{\max} - WEP_{\min}}{T} \right) \tag{36}$$

$$TDR = 1 - \frac{t^{1/p}}{T^{1/p}} \tag{37}$$

In Equation (37), t symbolizes the current iteration count, T is the aggregate quantity of iterations, and the max number of iterations was set to 200 in this study. $WEP_{\min}$ is the lower limit of wormhole existence probability, and $WEP_{\max}$ is the lower limit of wormhole existence probability, which are 0.2 and 1 in this research.

The exploration protocol employed in MOMVO [45] mirrors that of MVO, where solutions are advanced using white holes, black holes, and wormholes. However, MOMVO utilizes an additional formula to select options among areas of the archive that contain fewer entries for the roulette wheel, thereby improving the distribution of solutions for all targets within the archive. The formula is as follows:

$$P_i = c/N_i \tag{38}$$

in which c is a constant, which exceeds 1, and N_i is the count of results adjacent to the i-th solution.

The following section provides a comprehensive demonstration of the efficacy of these algorithms through experimental results. The optimal model optimized by each probabilistic prediction model and the multi-objective optimization algorithm are evaluated separately.

3. Experimental Setup and Results Analysis

This experiment employed a meticulously crafted research framework to predict gold prices (See Figure 1). The aim of our proposed method is to function as an early warning system for potential economic challenges, offering guidance amidst market ambiguity. Given the impact of recent epidemics on gold prices, our framework emphasizes a comprehensive evaluation of factors and a prudent selection of index variables. To enhance the economic applicability of the model, two variable selection methods that screen both "hard" and "soft" indicators were employed in this study. Furthermore, we utilized quantile regression (QR) and probabilistic forecasting algorithms (QRNN, QRLSTM, QRGRU, QRBiLSTM, QRBiGRU) for the gold price data. Finally, multi-objective optimization (MOALO and MOMVO) was integrated with quantile deep learning to fine-tune the convergence and width of the forecasting interval. The optimized model enhances forecasting accuracy and significantly improves the credibility of interval forecasting. This approach enhances our understanding and assessment of economic conditions and market uncertainty.

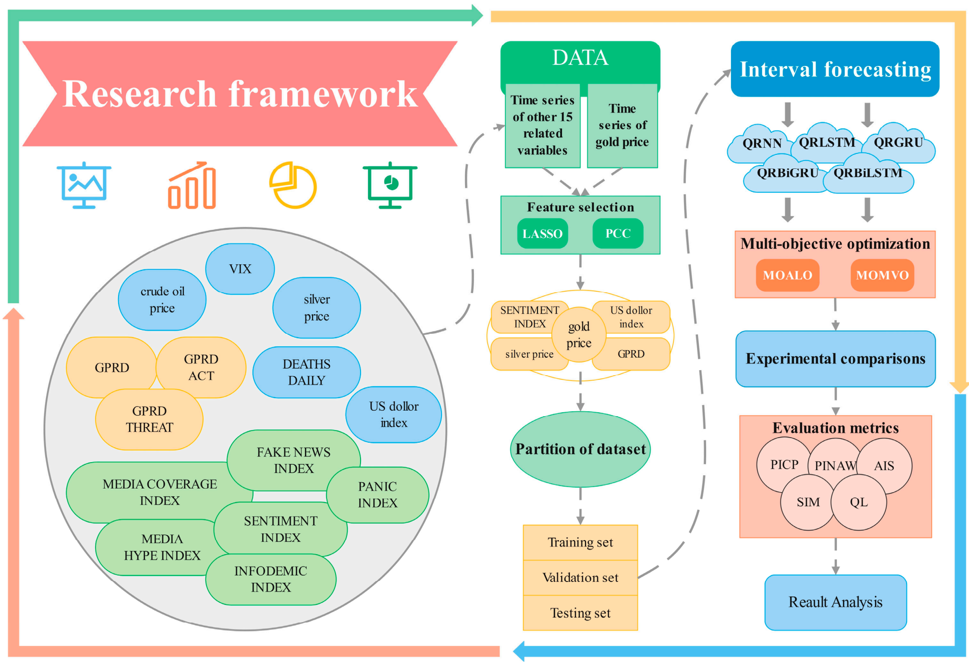

Figure 1. Research framework.

3.1. Data Collection

This study utilized a dataset comprising daily gold price data spanning from 1 January 2020 to 9 June 2023, covering 479 trading days. This dataset was divided as follows: 60% for training, 20% for validation, and 20% for test sets. Following an extensive literature research, 15 influencing factors were selected for this study, namely, the silver price, copper price, crude oil price, US Dollar Index, VIX Panic Index, three geopolitical risk factors (composite index Geopolitical Risk Index (GPRD), action index Geopolitical Risk Action Index (GPRD ACT), threat index Geopolitical Risk Threat Index (GPRDT HREAT)), Epidemic Deaths Daily, and six epidemic indices (Panic Index, Media Hype Index, Fake News Index, Sentiment Index, Infodemic Index, and Media Coverage Index). Silver prices, copper prices, crude oil prices, and the US Dollar Index are "hard" information, typical indicators of global economic activity. Crude oil prices are often seen as an indicator of the global economy's health due to oil's fundamental role in industrial production and transportation [46], and a stronger US dollar weakens the purchasing power of gold, leading to a decline in its price [3]. "Soft" information, which includes the Panic Index, Daily Epidemic Deaths, the Epidemic Index, and the Geopolitical Risk Index, reflects market uncertainty and risk perceptions. For example, the VIX Panic Index, which measures expectations of market volatility, tends to rise with market uncertainty, increasing demand for gold as a "haven" asset, and the Epidemic Index reflects the impact of global health crises, such as the new Crown Pneumonia, on the economy and market sentiment. The Geopolitical Risk Index is a composite, as geopolitical risk affects global economic stability and market confidence, which affects the price of gold, with political tensions driving investors towards safer assets such as gold. These factors have traditionally been recognized as important drivers of gold price dynamics, encompassing a wide range of economic, political, and market conditions affecting the demand for and supply of gold, thus providing a well-prepared forecast of gold price trends through a careful understanding and analysis of these factors. The gold, silver, copper, crude oil, US Dollar, and VIX panic indices are taken from the EWEB website (https://cn.investing.com/ (accessed on 18 June 2023)), the Geopolitical Risk Indexes from the geopolitical risk website (Geopolitical Risk (GPR) Index (matteoiacoviello.com (accessed on 18 June 2023))), and the epidemic indexes from RavenPack (https://coronavirus.ravenpack.com/ (accessed on 18 June 2023)). Figure 2 shows a trend chart, statistical indicators for the gold price data, and all the influencing factors.

3.2. Variable Selection

Variables that have little effect on the target variable can be filtered out to increase the precision of the model's predictions. In addition, a model that includes too many variables may lead to overfitting, i.e., the model is too complex and takes too much account of noisy or irrelevant data, resulting in a weakened ability to generalize to new samples. Variable screening allows the model to be simplified to include only variables with true explanatory power for the target variable, improving the model's interpretability and generalization ability. Therefore, the accurate selection of variables that significantly impact the target variables is crucial for building a valid and reliable forecasting model, especially for gold price forecasting.

In this study, LASSO was first chosen for variable screening, which left the variables of the silver price, Epidemic Deaths Daily, Media Hype Index, US dollar index, Sentiment Index, Panic Index, Infodemic Index, and GPRD. Then, the PCC was used for variable screening, which resulted in the price of silver, copper, Sentiment Index, VIX Panic Index, crude oil, US Dollar Index, GPRD ACT, and GPRD. The common features screened by the two variable screening methods, i.e., the Sentiment Index, Panic Index, US Dollar Index, GPRD, and silver price, were fed into the model for prediction. However, another issue to consider is the presence of multicollinearity between the influencing factors. Therefore, this study analyzed the correlation between the variables through the PCC methodology. Figure 3 shows the extent of association between the variables. The correlation between the Sentiment Index and Panic Index was too high for the characteristics we screened, and therefore, the Panic Index was disregarded in this study. Thus, the final inputs to the model in this study were the silver price, the Sentiment Index, the US Dollar Index, and the GPRD. In addition, the day's gold price data are also affected by the previous day's price, and first-order lagged data were also added as a feature input into the model.

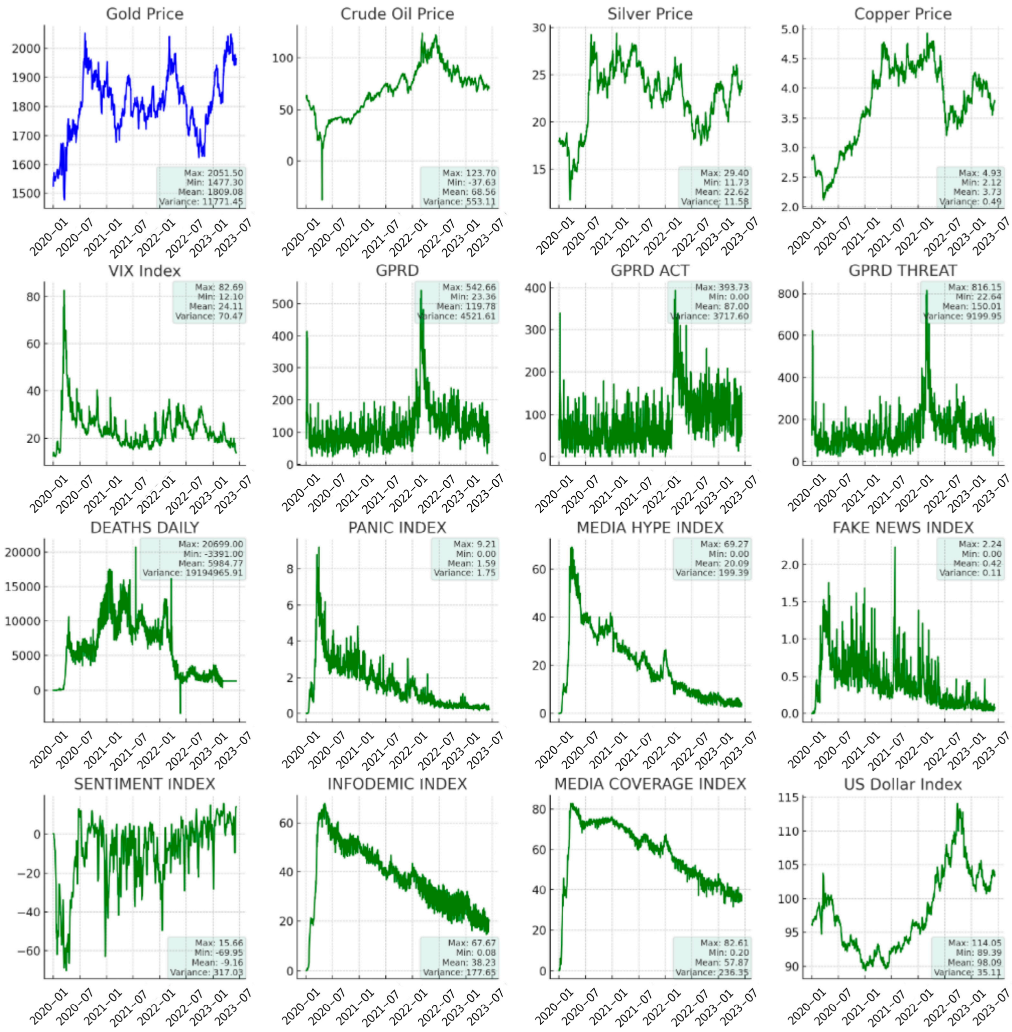

Figure 2. Visualization of all data.

In gold price forecasting, variables based on economic principles are of great importance in selecting predictor variables. To carefully choose variables that can predict the dynamics of the gold price, a comprehensive review of both established and unselected factors is necessary. For the variables screened in this study, the Sentiment Index is a measure of market sentiment and confidence, and in times of negative sentiment, investors tend to turn to safe assets such as gold to mitigate financial losses due to market volatility. The gold price is usually denominated in US dollars, and therefore, changes in the US dollar index directly influence the volatility of the gold price. The Geopolitical Risk Index summarizes the level of geopolitical tensions globally, and when the risks intensify, investors usually turn to safe assets such as gold. The precious metal's role as a store-of-value medium and market demand in the investment and industrial sectors has led to a close correlation between the price of silver and the price of gold.

On the other hand, unlike gold and silver, which are generally considered safe-haven assets, copper and crude oil prices are typically closely tied to the health of the global economy and industrial demand. The VIX Panic Index, which represents market volatility and investor sentiment, is not directly considered the price of gold. As a result, their correlation with gold is weaker. Similarly, although the Pandemic Index and the Geopolitical Risk Action and Threat Index reflect specific external shocks and global tensions, the broader Geopolitical Risk Index, which encompasses a more comprehensive range of geopolitical uncertainties, was chosen instead.

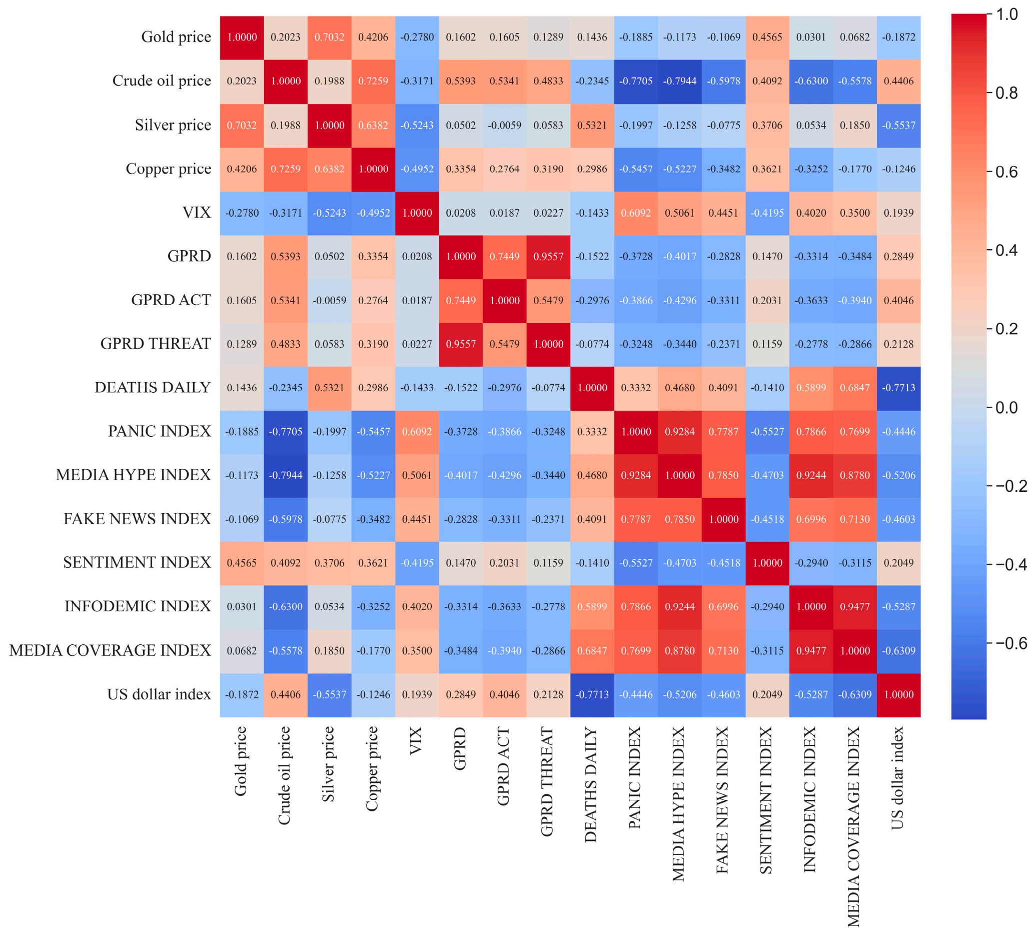

Figure 3. Characteristic correlation heat map.

3.3. Interval Forecasting Module Analysis

In Experiment 1, the performance of five quantile regression models (QRNN, QRLSTM, QRBiLSTM, QRGRU, and QRBiGRU) in forecasting gold prices was examined. The evaluation focused on assessing the reliability, utility, interval coverage, and interval width of these models using four evaluation metrics: Prediction Interval Coverage Probability (PICP), Prediction Interval Normalized Average Width (PINAW), Quantile Loss Metric, and Average Interval Score (AIS). The findings are displayed in Table 1 and Figure 4.

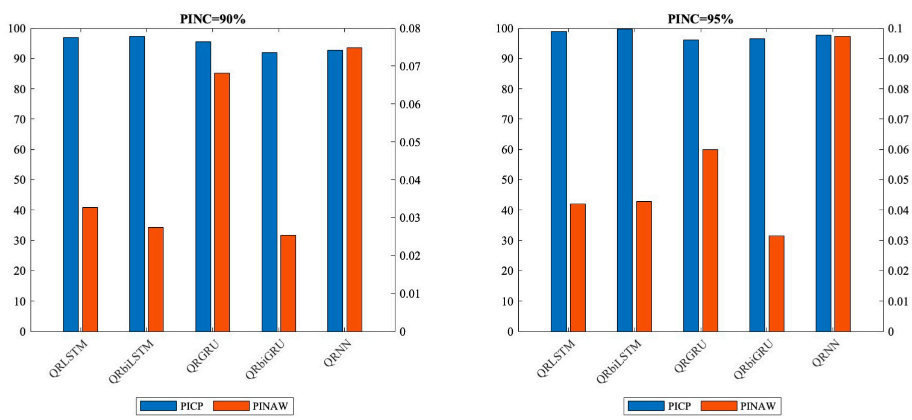

Figure 4. Comparison of PICP and PINAW.

Table 1. Comparison of evaluation metrics for basic probabilistic forecasting models.

			PINC = 90%		
Models	**PICP**	**PINAW**	**Quantile Loss (Upper Bound)**	**Quantile Loss (Lower Bound)**	**AIS**
QRNN	92.7757	0.0748	8.8672	5.8945	−59.0469
QRLSTM	96.9582	0.0327	1.9920	3.2460	−20.9538
QRBiLSTM	97.3384	0.0274	2.1124	2.1961	−17.2341
QRGRU	95.4373	0.0681	4.4170	6.1954	−42.4498
QRBiGRU	92.0152	0.0253	3.7081	2.3859	−24.3758
			PINC = 95%		
Models	**PICP**	**PINAW**	**Quantile Loss (Upper Bound)**	**Quantile Loss (Lower Bound)**	**AIS**
QRNN	97.7186	0.0973	5.4903	3.4743	−35.8586
QRLSTM	98.8593	0.0421	1.6091	1.6278	−12.9475
QRBiLSTM	99.6198	0.0429	1.2590	1.8716	−12.5227
QRGRU	96.1977	0.0599	1.9528	3.1812	−20.5361
QRBiGRU	96.5779	0.0315	2.7827	1.2459	−16.1144

Initially, the reliability of the prediction intervals was assessed using the PICP metric. A PICP value exceeding the nominal confidence level (PINC) indicates reliable forecasting. As shown in Table 1 and Figure 3, all models exhibit PICP values surpassing the corresponding PINC values, indicating reliable prediction across all models. Notably, the QRBiLSTM model performs exceptionally well, achieving the highest PICP values at PINC = 90% and PINC = 95% (97.3384% and 99.6198%, respectively), making it the most reliable model. The QRLSTM model closely follows, with PICP values of 96.9582% and 98.8593% at PINC = 90% and PINC = 95%, respectively.

Furthermore, the PINAW metric provides insights into the resolution and information content of the prediction intervals. A lower PINAW value indicates a narrower interval, offering a more detailed understanding of uncertainty. In this regard, the QRBiGRU model excels, achieving PINAW values of 0.0253 (PINC = 90%) and 0.0315 (PINC = 95%). The QRBiLSTM model secures the second position, with PINAW values of 0.0274 (PINC = 90%) and 0.0429 (PINC = 95%), and the QRNN model lags with the highest PINAW values of 0.0748 (PINC = 90%) and 0.0973 (PINC = 95%).

Lastly, a comprehensive assessment was conducted using the AIS and Quantile Loss metrics, considering both interval coverage and width. The evaluation reveals that the QRBiLSTM model achieves the lowest quantile loss value, closely followed by the QRLSTM model. Regarding AIS, the QRBiLSTM model demonstrates the highest values of −17.2341 and −12.5227 for PINC = 90% and PINC = 95%, respectively, with the QRLSTM model trailing slightly with AIS values of −20.9538 and −12.9475 for PINC = 90% and PINC = 95%. Considering the results from all interval evaluation metrics, it is evident that the QRBiLSTM model is the superior interval prediction model.

3.4. Optimization Module Analysis

In Experiment 2, the QRBiLSTM model, which demonstrated superior performance, was optimized using two metaheuristic algorithms: MOALO and MOMVO. The results obtained from these optimizations were compared with the pre-optimization outcomes. The findings are presented in Table 2 and Figure 5. For both the pre- and post-optimization models, the PICP values exceeded the designated PINC values, indicating reliable prediction intervals. When the nominal confidence level (PINC) was set at 90%, both optimization algorithms improved the PICP metrics. However, only the results optimized with the MOALO algorithm showed improvements in the PINAW value, quantile loss, and AIS. Specifically, the MOALO-optimized QRBiLSTM model achieved a PICP of 98.0989, a PINAW of 0.0254, an upper quartile loss of 2.2235, a lower quartile loss of 1.6824, and an

AIS of −15.6240. This marks a significant improvement over the pre-optimized QRBiLSTM model, which had a PICP of 97.3384, a PINAW of 0.0274, an upper quartile loss of 2.1124, a lower quartile loss of 2.1961, and an AIS of −17.2341. At PINC = 95%, QRBiLSTM optimized by MOALO resulted in a slight decrease in the PICP value to 95.0570 (but still higher than the PINC value), a slight improvement in the PINAW to 0.0421, better interquartile loss values of 1.3737 (upper bound) and 1.9935 (lower bound), and an AIS of −11.5581, which is an improvement of 0.9646 compared with the QRBiLSTM. However, the PINAW value of the QRBiLSTM model corrected for the MOMVO optimization error did not decrease but increased, and although the PICP value was slightly larger compared to the MOALO optimized result, the combined PICP and PINAW, i.e., the combined metrics AIS, were taken into account in the interval prediction, and the AIS value was not only better than that of the MOALO-QRBiLSTM but also smaller than the value of QRBiLSTM before optimization, and the prediction results were not improved. In conclusion, the MOALO-optimized QRBiLSTM model (i.e., MOALO- QRBiLSTM) performs well and is the best-performing model among the probabilistic prediction models.

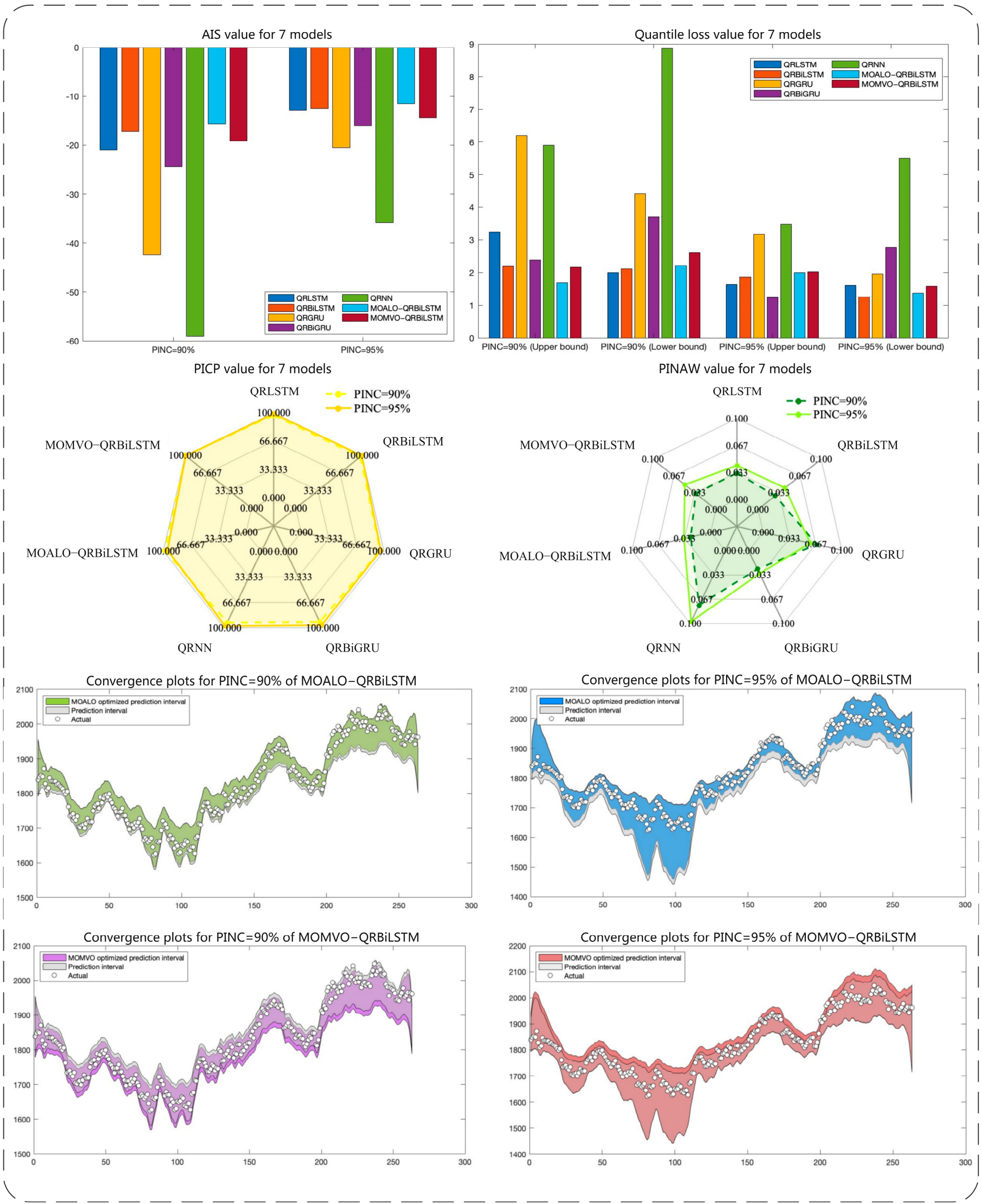

Figure 5. Comparison of all models.

Table 2. Comparison of evaluation indicators for optimization models.

			PINC = 90%		
Models	**PICP**	**PINAW**	**Quantile Loss (Upper Bound)**	**Quantile Loss (Lower Bound)**	**AIS**
MOALO-QRBiLSTM	98.0989	0.0254	2.2235	1.6824	−15.6240
MOMVO-QRBiLSTM	99.6189	0.0319	2.6110	2.1689	−19.1196
QRBiLSTM	97.3384	0.0274	2.1124	2.1961	−17.2341
			PINC = 95%		
Models	**PICP**	**PINAW**	**Quantile Loss (Upper Bound)**	**Quantile Loss (Lower Bound)**	**AIS**
MOALO-QRBiLSTM	95.0570	0.0421	1.3737	1.9935	−11.5581
MOMVO-QRBiLSTM	99.2395	0.0493	1.5760	2.0169	−14.3715
QRBiLSTM	99.6198	0.0429	1.2590	1.8716	−12.5227

4. Conclusions

In recent years, gold prices have undergone significant volatility, influenced by a complex web of factors, including trade tensions, global pandemics, geopolitical unrest, and economic crises. Gold is a crucial barometer of economic health, with its price fluctuations resonating deeply across the global economy. The stability and dynamics of the gold market are intricately linked to the broader economic vitality, impacting not only investment markets but also the macroeconomic stability and economic security of nations heavily invested in gold.

This study introduces a novel interval prediction framework for gold price forecasting. This framework, integrating multi-objective optimization with quantile deep learning, aims to improve the precision of gold price forecasts. The methodology unfolds in three phases: First, the study employed dimensionality reduction and variable selection methods to identify key factors influencing gold prices. Second, it leveraged QR deep-learning models for probabilistic and interval forecasting, thereby improving prediction accuracy and encompassing the uncertainty inherent in gold price movements. Then, fusing multi-objective optimization with quantile deep-learning methods, the convergence and width of prediction intervals were optimized simultaneously. This forecasting framework significantly boosts the accurate and reliable prediction of gold prices in a complex and often uncertain environment. The forecasts generated are not only robust but also highly precise, highlighting the effectiveness of our framework in delivering dependable and valuable insights for market analysts and economic strategists. Focusing on robustness and precision, our approach stands out in financial forecasting, providing a substantial edge.

This study substantially contributes to gold price forecasting and lays a foundation for further exploration and innovation in various domains requiring advanced predictive modeling. Future research could focus on tailoring this framework to specific market dynamics and exploring its adaptability in diverse environments, from commodities to other critical areas. This comprehensive approach sets a new benchmark for predictive modeling, especially in volatile market commodities like gold.

Author Contributions: Methodology, Y.W.; Software, Y.W.; Supervision, T.L.; Writing—original draft, Y.W.; Writing—review and editing, T.L. All authors have read and agreed to the published version of the manuscript.

Funding: This research was funded by the Humanities and Social Sciences of Ministry of Education Planning Fund, grant number 22YJA910004, National Key Research and Development Program of China 2023YFB3308903.

Data Availability Statement: The gold, silver, copper, crude oil, US Dollar, and VIX panic indices are available on the EWEB website (https://cn.investing.com/ (accessed on 18 June 2023)), the Geopolitical Risk Indexes are available on the geopolitical risk website (matteoiacoviello.com (accessed on 18 June 2023)), and the epidemic indexes are available on RavenPack (https://coronavirus.ravenpack.com/ (accessed on 18 June 2023)).

Acknowledgments: I would like to extend my deepest gratitude to Yan Xu for her invaluable guidance throughout the course of this research.

Conflicts of Interest: The authors declare no conflict of interest.

References

1. Pierdzioch, C.; Risse, M.; Rohloff, S. On the efficiency of the gold market: Results of a real-time forecasting approach. *Int. Rev. Financ. Anal.* **2014**, *32*, 95–108. [CrossRef]
2. Pierdzioch, C.; Risse, M.; Rohloff, S. The international business cycle and gold-price fluctuations. *Q. Rev. Econ. Financ.* **2014**, *54*, 292–305. [CrossRef]
3. Qian, Y.; Ralescu, D.A.; Zhang, B. The analysis of factors affecting global gold price. *Resour. Policy* **2019**, *64*, 101478. [CrossRef]
4. Chai, J.; Zhao, C.; Hu, Y.; Zhang, Z.G. Structural analysis and forecast of gold price returns. *J. Manag. Sci. Eng.* **2021**, *6*, 135–145. [CrossRef]
5. Zhang, P.; Ci, B. Deep belief network for gold price forecasting. *Resour. Policy* **2020**, *69*, 101806. [CrossRef]
6. Sharma, S.S. Can consumer price index predict gold price returns? *Econ. Model.* **2016**, *55*, 269–278. [CrossRef]
7. Wen, F.; Yang, X.; Gong, X.; Lai, K.K. Multi-scale volatility feature analysis and prediction of gold price. *Int. J. Inf. Technol. Decis. Mak.* **2017**, *16*, 205–223. [CrossRef]
8. Wang, G.; Meng, J.; Mo, B. Dynamic Volatility Spillover Effects and Portfolio Strategies among Crude Oil, Gold, and Chinese Electricity Companies. *Mathematics* **2023**, *11*, 910. [CrossRef]
9. Weng, F.; Zhang, H.; Yang, C. Volatility forecasting of crude oil futures based on a genetic algorithm regularization online extreme learning machine with a forgetting factor: The role of news during the COVID-19 pandemic. *Resour. Policy* **2021**, *73*, 102148. [CrossRef]
10. Su, M.; Cheng, D.; Xu, Y.; Weng, F. An improved BERT method for the evolution of network public opinion of major infectious diseases: Case Study of COVID-19. *Expert Syst. Appl.* **2023**, *233*, 120938. [CrossRef]
11. Xu, Y.; Liu, T.; Du, P. Volatility forecasting of crude oil futures based on Bi-LSTM-Attention model: The dynamic role of the COVID-19 pandemic and the Russian-Ukrainian conflict. *Resour. Policy* **2024**, *88*, 104319. [CrossRef]
12. Yang, C.; Abedin, M.Z.; Zhang, H.; Weng, F.; Hajek, P. An interpretable system for predicting the impact of COVID-19 government interventions on stock market sectors. *Ann. Oper. Res.* **2023**, *331*, 1–28. [CrossRef] [PubMed]
13. Umar, M.; Rubbaniy, G.; Iqbal, A.; Abbas Rizvi, S.K.; Xu, Y. Covid-19 and stock market liquidity: International evidence. *Econ. Res. Ekon. Istraživanja* **2023**, *36*, 2142257. [CrossRef]
14. Umar, M.; Xu, Y.; Mirza, S.S. The impact of Covid-19 on Gig economy. *Econ. Res. Ekon. Istraživanja* **2021**, *34*, 2284–2296. [CrossRef]
15. Atri, H.; Kouki, S.; Imen Gallali, M. The impact of COVID-19 news, panic and media coverage on the oil and gold prices: An ARDL approach. *Resour. Policy* **2021**, *72*, 102061. [CrossRef] [PubMed]
16. Polanco-Martínez, J.M. Dynamic relationship analysis between NAFTA stock markets using nonlinear, nonparametric, non-stationary methods. *Nonlinear Dyn.* **2019**, *97*, 369–389. [CrossRef]
17. Yang, C.; Zhang, H.; Weng, F. Effects of COVID-19 vaccination programs on EU carbon price forecasts: Evidence from explainable machine learning. *Int. Rev. Financ. Anal.* **2024**, *91*, 102953. [CrossRef]
18. Van Houdt, G.; Mosquera, C.; Nápoles, G. A review on the long short-term memory model. *Artif. Intell. Rev.* **2020**, *53*, 5929–5955. [CrossRef]
19. Weng, F.; Chen, Y.; Wang, Z.; Hou, M.; Luo, J.; Tian, Z. Gold price forecasting research based on an improved online extreme learning machine algorithm. *J. Ambient Intell. Humaniz. Comput.* **2020**, *11*, 4101–4111. [CrossRef]
20. Alameer, Z.; Abd Elaziz, M.; Ewees, A.A.; Ye, H.; Jianhua, Z. Forecasting gold price fluctuations using improved multilayer perceptron neural network and whale optimization algorithm. *Resour. Policy* **2019**, *61*, 250–260. [CrossRef]
21. Mirjalili, S.; Lewis, A. The whale optimization algorithm. *Adv. Eng. Softw.* **2016**, *95*, 51–67. [CrossRef]
22. Mu, L.; Wang, Z.; Wu, D.; Zhao, L.; Yin, H. Prediction and evaluation of fuel properties of hydrochar from waste solid biomass: Machine learning algorithm based on proposed PSO–NN model. *Fuel* **2022**, *318*, 123644. [CrossRef]
23. Karimi, H.; Yousefi, F.; Rahimi, M.R. Correlation of viscosity in nanofluids using genetic algorithm-neural network (GA-NN). *Heat Mass Transf.* **2011**, *47*, 1417–1425. [CrossRef]
24. Li, G.Q.; Xu, S.W.; Li, Z.M.; Sun, Y.G.; Dong, X.X. Using quantile regression approach to analyze price movements of agricultural products in China. *J. Integr. Agric.* **2012**, *11*, 674–683. [CrossRef]
25. Liu, D.; Li, Z. Gold price forecasting and related influence factors analysis based on random forest. In Proceedings of the Tenth International Conference on Management Science and Engineering Management; Springer: Singapore, 2017; pp. 711–723. [CrossRef]

26. Tian, C.; Hao, Y. Point and interval forecasting for carbon price based on an improved analysis-forecast system. *Appl. Math. Model.* **2020**, *79*, 126–144. [CrossRef]
27. Wang, J.; Wang, S.; Li, Z. Wind speed deterministic forecasting and probabilistic interval forecasting approach based on deep learning, modified tunicate swarm algorithm, and quantile regression. *Renew. Energy* **2021**, *179*, 1246–1261. [CrossRef]
28. Mombeini, H.; Yazdani-Chamzini, A. Modeling gold price via artificial neural network. *J. Econ. Bus. Manag.* **2015**, *3*, 699–703. [CrossRef]
29. Yurtsever, M. Gold price forecasting using LSTM, Bi-LSTM and GRU. *Avrupa Bilim Teknol. Derg.* **2021**, *31*, 341–347. [CrossRef]
30. Wang, S.; Wang, X.; Wang, S.; Wang, D. Bi-directional long short-term memory method based on attention mechanism and rolling update for short-term load forecasting. *Int. J. Electr. Power Energy Syst.* **2019**, *109*, 470–479. [CrossRef]
31. Shu, W.; Cai, K.; Xiong, N.N. A short-term traffic flow prediction model based on an improved gate recurrent unit neural network. *IEEE Trans. Intell. Transp. Syst.* **2021**, *23*, 16654–16665. [CrossRef]
32. Li, G.; Wu, D.C.; Zhou, M.; Liu, A. The combination of interval forecasts in tourism. *Ann. Tour. Res.* **2019**, *75*, 363–378. [CrossRef]
33. Wang, J.; Zhou, Y.; Jiang, H. A novel interval forecasting system based on multi-objective optimization and hybrid data reconstruct strategy. *Expert Syst. Appl.* **2023**, *217*, 119539. [CrossRef]
34. Zhang, Y.; Ma, F.; Wang, Y. Forecasting crude oil prices with a large set of predictors: Can LASSO select powerful predictors? *J. Empir. Financ.* **2019**, *54*, 97–117. [CrossRef]
35. Baak, M.; Koopman, R.; Snoek, H.; Klous, S. A new correlation coefficient between categorical, ordinal and interval variables with Pearson characteristics. *Comput. Stat. Data Anal.* **2020**, *152*, 107043. [CrossRef]
36. Weng, F.; Zhu, J.; Yang, C.; Gao, W.; Zhang, H. Analysis of financial pressure impacts on the health care industry with an explainable machine learning method: China versus the USA. *Expert Syst. Appl.* **2022**, *210*, 118482. [CrossRef]
37. Taylor, J.W. A quantile regression neural network approach to estimating the conditional density of multiperiod returns. *J. Forecast.* **2000**, *19*, 299–311. [CrossRef]
38. Liu, F.; Umair, M.; Gao, J. Assessing oil price volatility co-movement with stock market volatility through quantile regression approach. *Resour. Policy* **2023**, *81*, 103375. [CrossRef]
39. He, Y.; Cao, C.; Wang, S.; Fu, H. Nonparametric probabilistic load forecasting based on quantile combination in electrical power systems. *Appl. Energy* **2022**, *322*, 119507. [CrossRef]
40. Ying, H.; Deng, C.; Xu, Z.; Huang, H.; Deng, W.; Yang, Q. Short-term prediction of wind power based on phase space reconstruction and BiLSTM. *Energy Rep.* **2023**, *9*, 474–482. [CrossRef]
41. Zhang, C.; Ji, C.; Hua, L.; Ma, H.; Nazir, M.S.; Peng, T. Evolutionary quantile regression gated recurrent unit network based on variational mode decomposition, improved whale optimization algorithm for probabilistic short-term wind speed prediction. *Renew. Energy* **2022**, *197*, 668–682. [CrossRef]
42. Mirjalili, S. The ant lion optimizer. *Adv. Eng. Softw.* **2015**, *83*, 80–98. [CrossRef]
43. Mirjalili, S.; Jangir, P.; Saremi, S. Multi-objective ant lion optimizer: A multi-objective optimization algorithm for solving engineering problems. *Appl. Intell.* **2017**, *46*, 79–95. [CrossRef]
44. Mirjalili, S.; Mirjalili, S.M.; Hatamlou, A. Multi-verse optimizer: A nature-inspired algorithm for global optimization. *Neural Comput. Appl.* **2016**, *27*, 495–513. [CrossRef]
45. Mirjalili, S.; Jangir, P.; Mirjalili, S.Z.; Saremi, S.; Trivedi, I.N. Optimization of problems with multiple objectives using the multi-verse optimization algorithm. *Knowl. -Based Syst.* **2017**, *134*, 50–71. [CrossRef]
46. Ghalayini, L.; Farhat, S. Modeling and Forecasting Gold Prices. *Res. Sq.* **2020**. [CrossRef]